Technical Notes

TECHNICAL NOTES are short manuscripts describing new developments or important results of a preliminary nature. These Notes cannot exceed 6 manuscript pages and 3 figures; a page of text may be substituted for a figure and vice versa. After informal review by the editors, they may be published within a few months of the date of receipt. Style requirements are the same as for regular contributions (see inside back cover).

A Nonlinear Guidance Scheme for Intercept Mission

ROBERT F. WEBBER* AND GIOVANNI BONFANTI†
Martin Marietta Corporation, Orlando, Fla.

Introduction

A GUIDANCE law has been devised to reduce the airborne computational load associated with forward prediction (by numerical integration) of the state vectors of both interceptor and target. The scheme provides a solution for the guidance command in essentially closed-form and considers the nonlinear effects of maneuver-induced drag on the interceptor. The maneuver histories derived are optimal in nature, in the sense that they maximize the interceptor velocity at the time of intercept, thus minimizing the energy loss due to drag.

Equations of Motion and Guidance Law

Consider a right-handed coordinate frame (xyz) whose origin coincides with the predicted intercept point, and its orientation is such that the abscissa is always in the direction of the interceptor velocity vector $\mathbf{V}_I$ (Fig. 1). To maintain this condition, the xyz frame must rotate at a rate ω identical to the angular rotation of the velocity vector of the interceptor.

Assume that the motions are limited to one plane. Let the interceptor be at a distance $\mathbf{R}_p$ from the predicted intercept point (i.e., the origin of xyz) and moving with velocity $\mathbf{V}_I$ and acceleration $\mathbf{a}$. Call $(\mathbf{i}, \mathbf{j}, \mathbf{k})$ the orthogonal set of unit vectors corresponding to the xyz frame, then, referred to this frame:

$$\mathbf{R}_p = R_1\mathbf{i} + R_2\mathbf{j}, \quad \mathbf{V}_I = V_1\mathbf{i} + 0\mathbf{j}, \quad \mathbf{a} = a_1\mathbf{i} + a_2\mathbf{j}, \quad \boldsymbol{\omega} = \omega\mathbf{k}$$

Note that $\mathbf{V}_2 = 0$ because of the selection of this particular frame.

As viewed by an observer in the xyz frame, the kinematics of the interceptor are described by:

$$\dot{R}_1 = V_1 + \omega R_2, \quad \dot{R}_2 = -\omega R_1, \quad \dot{V}_1 = a_1 \tag{1a}$$

$$\dot{V}_2 = a_2 - \omega V_1 = 0 \Rightarrow \omega = a_2/V_1 \tag{1b}$$

For a nonthrusting vehicle with an assumed parabolic $C_D - C_L$ relationship, a_1 and a_2 are simply the drag and lift components of acceleration given below, where ρ is the atmospheric density, S_π the reference area, W the weight, and A the induced drag coefficient.

$$a_1 = -\rho S_\pi V_1^2(C_{D_o} + AC_L^2)/2W, \quad a_2 = \rho S_\pi V_1^2 C_L/2W \tag{2}$$

To derive the optimal navigational constant to maximize the interceptor velocity at intercept, a proportional navigation type of control will be assumed such that with constant K: $KR_1/R_2 = \dot{R}_1/\dot{R}_2$. With R_{10} and R_{20} as the initial values of R_1 and R_2, respectively, the solution of this equation is:

$$R_2 = CR_1^K, \quad C = R_{20}R_{10}^{-K} \tag{3}$$

Then, using Eq. (1), an expression for the lift acceleration necessary to drive R_2 to zero is obtained

$$a_2 = -KR_2V_1^2/(R_1^2 + KR_2^2) \tag{4}$$

Assuming that the interceptor is in a near-collision course with its target, it follows that $R_2/R_1 \ll 1$ and for reasonable values of K (i.e., $K < 10$), $K(R_2/R_1)^2 \ll 1$, then defining $B_D = \rho S_\pi C_{D_o}/2W$ and $B_I = 2WA/\rho S_\pi$, it may be shown that

$$\dot{V}_1 \approx -V_1^2(B_D + K^2B_IC^2R_1^2) \text{ and } \dot{R}_1 \approx V_1 \tag{5}$$

$$dV_1/V_1 = (-B_D - B_IK^2C^2R_1^{2K-4})\,dR_1 \tag{6}$$

Using the expression for C given in Eq. (3) and the fact that at intercept $R_1 = 0$, both sides of Eq. (6) may be integrated from V_{10} to V_1 and from R_{10} to R_1, respectively, to obtain an expression for the final value of $V_1(\triangleq V_{1f})$ in the form of $\ln(V_{1f}/V_{10}) = B_DR_{10} + (B_IR_{20}^2R_{10}^{-3}K^2)/(2K - 3)$. Since ln is a monotonic function, to maximize V_{1f}, it is only necessary to maximize $\ln V_1f/V_{10}$. Thus, setting the derivative of (6) with respect to K equal to zero: $K(K - 3)/(2K - 3)^2 = 0$. For $K \neq 1.5$ this equation becomes $K(K - 3) = 0$, or $K = 0,3$.

The value of $K = 0$ corresponds to the trivial case of no maneuver and therefore, in general, no intercept. Thus, the solution $K = 3$ is the one that leads to maximum velocity at intercept. To compute the guidance command as given by Eq. (4), it is necessary to know R_1 and R_2 or, in other words, the location of the origin of the xyz frame relative to the interceptor position. Since this origin corresponds to the predicted intercept point, it follows that the re-entry vehicle must arrive at that point simultaneously with the interceptor. Knowing the equations of motion of both the interceptor and its target it should be possible to solve for their position as a function of time and find that point in space that can be reached by both bodies in equal amounts of time. To avoid having to integrate the differential equations during the actual implementation of the proposed guidance scheme, a method is presented that allows the solution of the pertinent equations down to a point at which no integration is necessary. Unfortunately, this point does not quite yield an explicit solution and some interative process must be invoked. Yet, as far as the mechanization is concerned, the computational requirements (memory and time) are expected to be considerably less than those imposed by the equivalent integration scheme.

It has already been assumed that the interceptor is in a near-collision course, i.e. $R_2 \ll R_1$; thus it will, at this point, be

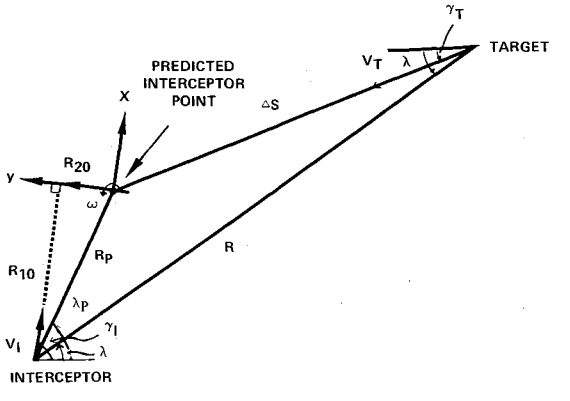

Fig. 1 Engagement geometry.

Presented as Paper 71-916 at the AIAA Guidance, Control and Flight Mechanics Conference, Hofstra University, Hempstead, N. Y., August 16–18, 1971, submitted September 29, 1971; revision received March 15, 1970. This work was partially supported by ABMDA under contract DAHC60-69-C-0095.

Index categories: Launch Vehicle and Missile Guidance Systems; Missile Systems; Navigation, Control, and Guidance Theory.

* Senior Research Scientist, Guidance and Control Department, Systems Engineering.

† Staff Engineer, Guidance and Control Department, Systems Engineering.

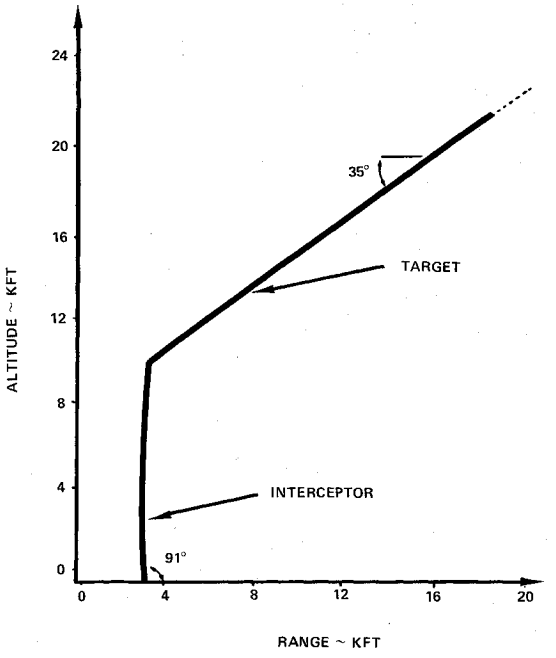

Fig. 2 Engagement results.

assumed that the induced drag deceleration resulting from the maneuver necessary to steer the interceptor into a collision course is small compared to the zero-lift drag deceleration. This assumption allows direct integration of Eq. (5), yielding the following Approximate solution:

$$\hat{V}_1 = V_{10}/(B_D V_{10} t + 1) \text{ and} \tag{7a}$$

$$\hat{R}_1 = R_{10} + \int_0^t \hat{V}_1 dt = R_{10} + B_D{}^{-1} \ln(V_{T_o} B_D t + 1) \tag{7b}$$

To obtain a better solution to Eqs. (5), consider the first variation given by:

$$V_1 = \hat{V}_1 + \varepsilon_V \text{ and } R_1 = \hat{R}_1 + \varepsilon_R \tag{8}$$

Equations (8) are a solution of Eq. (5) if they satisfy those equations; that is, if for $K = 3$:

$$\dot{\varepsilon}_V = -9 B_I C^2 \hat{V}_1{}^2 \hat{R}_1{}^2, \quad \dot{\varepsilon}_R = \varepsilon_V \tag{9}$$

where $\hat{V}_1$ and R_1 are given by Eqs. (7).

At the final time t_f corresponding to intercept, it must be true that $R_1 = 0$. Then, defining the normalized time as $\tau = B_D V_{10} t + 1$ and $\tau_f = B_D V_{10} t_f + 1$, integration of Eqs. (9) combined with Eqs. (7) and (8) yields

$$0 = R_{10} B_D + \ln \tau_f + 9 C^2 B_I B_D{}^{-3} \{[(R_{10} B_D + 1)^2 + 1] \cdot (1 - \tau_f + \ln \tau_f) + (R_{10} B_D + 1) \ln^2 \tau_f + \tfrac{1}{3} \ln^3 \tau_f\} \tag{10}$$

This equation could be solved for R_{10} as a function of τ_f (and therefore for t_f), but for the present analysis it is sufficient to consider it as one equation in two unknowns, namely R_{10} and t_f. It is now necessary to obtain another equation relating the same two variables to make a solution, although not explicit, obtainable by some iterative scheme. This additional equation is derived from the target equations.

For a nonmaneuvering target, and ignoring the effects of gravity, the equations of motion may be expressed as

$$\gamma_T = \gamma_{T0} = \text{const and } \dot{V}_T = -B_T V_T{}^2, \quad B_T = \rho_T / 2\beta_T \tag{11}$$

Without loss of generality, the time origin may be taken at t_0, i.e., $t_0 = 0$, and assuming ρ_T to be constant over the region of interest, Eq. (11), rewritten as $dV_T/V_T{}^2 = -B_T\, dt$, may be integrated from V_{T0} to V_T and from $t_0 = 0$ to t, to obtain V_T as function of time. This will in turn be used to compute the distance ΔS traveled along the direction of $\mathbf{V}_T$ in time t

$$\Delta S = \int_0^t V_T\, dt = B_T{}^{-1} \ln(V_{T0} B_T t + 1) \tag{12}$$

From the geometry of Fig. 1

$$R \cos \lambda - \Delta S \cos \gamma_T = R_P \cos \lambda_P \tag{13a}$$

$$R \sin \lambda - \Delta S \sin \gamma_T = R_P \sin \lambda_P \tag{13b}$$

Using the law of cosines

$$R_P{}^2 = R^2 + (\Delta S)^2 - 2R\Delta S \cos(\lambda - \gamma_T) \tag{14}$$

Also

$$R_{10} = -R_P \cos(\gamma_I - \lambda_P) \tag{15a}$$

$$R_{20} = R_P \sin(\gamma_I - \lambda_P) \tag{15b}$$

Assuming the heading angle of the interceptor and the target (γ_I and γ_T) and the relative quantities (R and λ) are known (observed), Eq. (15a) aided by (12), (13a and b), and (14), yields the equation relating R_{10} and t that, for $t = t_f$, can be used in conjunction with Eq. (10) to form a set of two equations in two unknowns, R_{10} and t_f, it is obvious that obtaining an explicit solution for these two variables is, to say the least, cumbersome if at all possible and an iterative scheme is therefore suggested: 1) Select as the initial value of t_f some easily computed quantity, such as $\hat{t}_f = |\text{Range/Range Rate}|$; 2) substitute $t = \hat{t}_f$ in (12) to obtain ΔS; 3) Obtain $R_P \sin \lambda_P$ and $R_P \cos \lambda_P$ from Eqs. (13); 4) Compute R_{10} from (15a) from (15b); 5) Let $\hat{t}_f = t_f$ and compute $\tau_f = B_D V_{10} t_f + 1$; 6) Substitute these values for R_{10}, R_{20} and τ_f in (10).

Unless R_{10} and τ_f are the proper values, Eq. (10) will not be satisfied; that is, a nonzero value will be obtained. Recalling that R_{10} is a negative quantity, it follows by inspection that a negative answer at step 4) implies that the estimate of τ_f, and therefore $\hat{t}_f$, was too small, and vice versa. After a suitable form of correcting $\hat{t}_f$ is selected, the outlined steps are repeated until the desired accuracy on $\hat{t}_f$, and therefore R_{10}, are obtained. At this point, the desired acceleration command may be computed from Eq. (4), with $K = 3$, i.e., $a_2 = -3R_{20} V_1{}^2 / (R_{10}{}^2 + 3R_{20}{}^2)$.

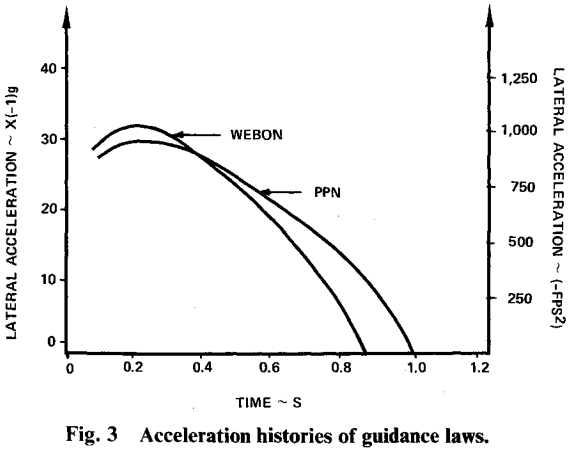

Fig. 3 Acceleration histories of guidance laws.

Simulation

The presented guidance scheme, hereafter referred to as WEBON guidance, was tested and compared against predictive proportional navigation (PPN) by means of a digital simulation. In both schemes the guidance command drives an estimated miss distance to zero, that is, a predicted intercept point is found and the interceptor is guided to that point. This prediction is updated at fixed intervals of time during flight and each time a new guidance command is transmitted to the autopilot of the interceptor. The difference between the two schemes is that PPN requires forward integration of the simulated equations of motion, for both vehicles, and for every guidance command generated, whereas the presented scheme simply requires the solution of algebraic equations.

The cases used to test WEBON guidance required extreme extreme accuracy in the presence of poor intercept geometry. The philosophy being that if the iterative process proposed for the solution of Eq. (10) converged adequately for the cases selected, it would be safe to assume adequate convergence under

Table 1 Comparison of guidance laws

Time, sec	Acceleration command, fps		Time-to-go, sec		Number of iterations
	WEBON	PPN	WEBON	PPN	
0.1	−934	−873	0.9530	0.9574	4
0.2	−1,030	−961	0.8539	0.8576	4
0.3	−983	−933	0.7547	0.7572	4
0.4	−882	−864	0.6554	0.6568	4
0.5	−757	−774	0.5559	0.5565	4
0.6	−599	−670	0.4562	0.4563	3
0.7	−404	−552	0.3564	0.3563	3
0.8	−164	−419	0.2565	0.2564	3
0.9	163	−257	0.1566	0.1565	3
1.0	633	58	0.0566	0.0565	2

At intercept: Guidance scheme	Time, sec	g-s	Miss, ft
WEBON	1.057	18.5	1.5
PPN	1.057	19.4	1.7

less stringent conditions. Thus, engagements between a very fast interceptor (~ 10 kfps) and a target with velocity superiority of up to 2:1 were simulated. The geometry of an actual engagement simulated is depicted in Figure 2. The origin of the coordinate frame is at an altitude of approximately 25 kft and the total duration of the engagement is just over one second. Thus WEBON was tested here in the role of homing guidance. For economical reasons, only deterministic cases were considered here.

Results

Trajectories for a simulated engagement are shown in Fig. 2. The corresponding interceptor acceleration command histories obtained with PPN as well as WEBON guidance are shown in Fig. 3. Table 1 presents a numerical comparison of these guidance commands showing, in addition, a comparison of the time-to-go estimates as a function of engagement time, and the number of iterations required for convergence by the presented guidance scheme.

In spite of the comparison against a very sophisticated guidance scheme, the results obtained were encouraging. The energy loss due to drag was, as in the case shown in Table 1, reduced in all cases considered. This reduction would be more pronounced against simpler guidance schemes, such as proportional navigation. The fact that atmospheric density had to be assumed constant to obtain the closed form solution presented may account for part of the difference shown in the initial estimates of $\hat{t}_f$, but this did not prove detrimental.

Mechanical Behavior of Fiber Reinforced Cylindrical Shells

J. PADOVAN* AND J. LESTINGI†
University of Akron, Akron, Ohio

TO date, the effects of material anisotropy on the static behavior of cylindrical shells has been studied by several investigators.[1-4] In all of these analyses though, no numerical results are available for the case of nonsymmetric loading of such shells. The present Note studies the mechanical response of a statically loaded, fiber-reinforced cylindrical shell with arbitrary boundary conditions. Specifically, the effects of fiber orientation on the shell stress, strain and displacement fields of the cylinder are discussed in detail. Since the cylinder is fiber-reinforced, the material properties are characterized as a generalized Hookean material characteristic of anisotropic shell theory.

The position of a point of a cylindrical shell is given by β the circumferential variable, x the axial distance, and z the coordinate normal to the middle surface. Furthermore, R is the radius of the cylinder, H the thickness, and L the length. Since the cylinder coordinates (x, β) generally do not line up with the fiber directions, the 3-D constitutive equations will have certain anisotropic compliances included. As shear deformation is admitted in the present analysis, the constitutive equations appropriate to the cylindrical shell have the form

$$\begin{bmatrix} \sigma_{xx} \\ \sigma_{\beta\beta} \\ \sigma_{x\beta} \\ \sigma_{\beta z} \\ \sigma_{zx} \end{bmatrix} = \begin{bmatrix} E_{11} & E_{12} & E_{13} & 0 & 0 \\ & E_{22} & E_{24} & 0 & 0 \\ & & E_{44} & 0 & 0 \\ & & & E_{55} & E_{56} \\ & & & & E_{66} \end{bmatrix} \begin{bmatrix} \varepsilon_{xx} \\ \varepsilon_{\beta\beta} \\ \varepsilon_{x\beta} \\ \varepsilon_{\beta z} \\ \varepsilon_{zx} \end{bmatrix} \tag{1}$$

where $\sigma_{xx}, \ldots$ and $\varepsilon_{xx}, \ldots$ are 3-D stresses and strains.

Since shear deformation is admitted, the shell strains and stresses are given by

$$\varepsilon_{xx} = u^{(0)}_{,x} + z u^{(1)}_{,x} \tag{2a}$$

$$\varepsilon_{\beta\beta} = [1/(R+z)]v^{(0)}_{,\beta} + [z/(R+z)]v^{(1)}_{,\beta} + [1/(R+z)]w^{(0)} \tag{2b}$$

$$\varepsilon_{x\beta} = [1(R+z)]u^{(0)}_{,\beta} + [z/(R+z)]u^{(1)}_{,\beta} + v^{(0)}_{,x} + z v^{(1)}_{,x} \tag{2c}$$

$$\varepsilon_{\beta z} = [1/(R+z)]w^{(0)}_{,\beta} - [1/(R+z)]v^{(0)} - [z/(R-z)]v^{(1)} + v^{(1)} \tag{2d}$$

$$\varepsilon_{zx} = u^{(1)} + w^{(0)}_{,x} \tag{2e}$$

$$\{\sigma^{(0)}_{xx}, \sigma^{(0)}_{x\beta}, \sigma^{(0)}_{zx}; \sigma^{(0)}_{xx}, \sigma^{(1)}_{x\beta}\} = < (\sigma_{xx}, \sigma_{x\beta}, \sigma_{zx})(R+z)(1; z) > \tag{3a}$$

$$\{\sigma^{(0)}_{\beta x}, \sigma^{(0)}_{\beta\beta}, \sigma^{(0)}_{\beta z}; \sigma^{(1)}_{\beta x}, \sigma^{(1)}_{\beta\beta}\} = < (\sigma_{\beta x}, \sigma_{\beta\beta}, \sigma_{\beta x})(1; z) > \tag{3b}$$

For notational convenience $(\ )_{,x}$ and $(\ )_{,\beta}$ denote partial differentiation with respect to x and β and $< >$ is defined by‡

$$< > = \int_{-H/2}^{+H/2} (\ )\, dz \tag{4}$$

Furthermore, $u^{(0)}$, $v^{(0)}$, and $w^{(0)}$ are the shell displacements of the middle surface in the x, β and z directions and $u^{(1)}$, $v^{(1)}$ are the rotations of the normal to the middle surface in the x and β directions. For the material properties characterized by Eq. (1), the displacement equilibrium equations can be written as[6]

$$B_1\zeta_{,xx} + B_2\zeta_{,\beta\beta} + B_3\zeta_{,x\beta} + B_4\zeta_{,x} + B_5\zeta_{,\beta} + B_6\zeta + \mathbf{F} = \mathbf{0} \tag{5}$$

where the coefficients B_l, $l = 1, 2, \ldots, 6$ are five by five matrices such that B_1, B_2, B_3 and B_6 are Hermitian while B_4 and B_5 are

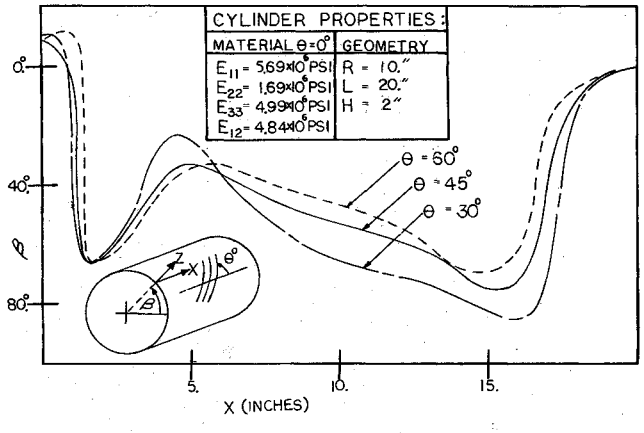

Fig. 1 Loci of the maximum value of $\sigma^{(1)}_{xz}$ for several values of θ.

Received December 1, 1971; revision received April 19, 1972.
Index categories: Structural Composite Materials (Including Coatings); Structural Static Analysis.

* Assistant Professor of Mechanical Engineering.
† Associate Professor of Civil Engineering.

‡ The integration defined by Eq. (4) is performed in the manner of Flügge second order theory.[5]